Journal of Cleaner Production 278 (2021) 123212

Contents lists available at ScienceDirect

Journal of Cleaner Production

journal homepage: www.elsevier.com/locate/jclepro

Role of redox-active biochar with distinctive electrochemical properties to promote methane production in anaerobic digestion of waste activated sludge

Yanwen Shen [a, 1], Yamei Yu [a, 1], Yue Zhang [a], Meltem Urgun-Demirtas [b], Haiping Yuan [a], Nanwen Zhu [a, c, *], Xiaohu Dai [d]

[a] School of Environmental Science and Engineering, Shanghai Jiao Tong University, 800 Dongchuan Road, Shanghai, 200240, China
[b] Energy Systems Division, Argonne National Laboratory, 9700 S. Cass Avenue, Lemont, IL, 60439, United States
[c] Shanghai Institute of Pollution Control and Ecological Security, 1239 Siping Road, Shanghai, 200092, China
[d] State Key Laboratory of Pollution Control and Resources Reuse, College of Environmental Science and Engineering, Tongji University, 1239 Siping Road, Shanghai, 200092, China

ARTICLE INFO

Article history:
Received 30 October 2019
Received in revised form
2 June 2020
Accepted 5 July 2020
Available online 7 August 2020

Handling editor: Yutao Wang

Keywords:
Redox-active biochar
Waste activated sludge
Anaerobic digestion
Interspecies electron transfer
Syntrophy

ABSTRACT

Biochar has been reported as an effective additive to improve methane production during anaerobic digestion (AD). However, the mechanism for such a stimulatory impact remains unclear. Here we investigated the capability of three pyrolytic biochars with distinctive electrochemical properties (BC300, BC500, BC700) to promote methanogenic performance of anaerobic digesters treating waste activated sludge (WAS). The cumulative methane production and the maximum methane production rate were increased by 46.9% and 181.6%, respectively, with BC300 amendment. By characterizing the electrochemical properties of biochar, we found out that methane production in AD of sludge was positively correlated to biochar's electron-donating capacity (EDC) rather than its bulk electrical conductivity. These results indicate that the electron transfer mediated by the redox-active functional groups may prevail over the direct electron migration as the predominant mechanism to facilitate interspecies electron transfer in syntrophic communities for enhanced methanogenesis. Microbial community analysis suggests that biochar enriched *Methanosarcina* and *Methanobacterium*. Overall, this study shows that functional groups-mediated electron transfer contributes greatly to the improved methane production in WAS digester with biochar amendment.

1. Introduction

Municipal wastewater contains up to 10 times more energy, most in the form of organic matters, than the energy required to clean it (Heidrich et al., 2011). Anaerobic digestion (AD) is one of the proven biotechnologies deployed on large scale for simultaneous recovery of the energy embodied in wastewater and waste activated sludge (WAS) stabilization, during which organic matters are degraded and eventually converted to biogas that can be further upgraded to biomethane. Biomethane is a fungible renewable fuel under the expanded Renewable Fuel Standard by the US Environmental Protection Agency and plays an important role in the current biofuel industry (Angenent et al., 2018; Shen et al., 2015a).

From the perspective of microbiology, methane production in AD process mainly depends on the syntrophic interaction between bacteria and archaea (Stams and Plugge, 2009). Fermentative bacteria decompose complex organic compounds and produce intermediate metabolites, primarily volatile fatty acids (VFAs), and then acetogens further degrade them into acetate, hydrogen (H_2) and carbon dioxide (CO_2). This process is not thermodynamically feasible, unless hydrogenotrophic methanogens consume H_2 to reduce its partial pressure. Methanogenic consortia live in syntrophy to degrade organic compounds together. Interspecies electron transfer (IET) mediated by H_2 or formate as electron shuttles is the best-known mechanism for energy exchange in methanogenic consortia (Sieber et al., 2012). Yet this IET is limited by the

* Corresponding author. 513 Environmental Science Building, Shanghai Jiao Tong University, 800 Dongchuan Road, Shanghai 200240, China.
E-mail address: nwzhu@sjtu.edu.cn (N. Zhu).
[1] These authors contributed equally.

https://doi.org/10.1016/j.jclepro.2020.123212
0959-6526/

mediator's diffusion flux, which may become rate-limiting in AD, since the concentration gradient of H_2 or formate is usually small to maintain the thermodynamic feasibility (Storck et al., 2016).

Biochar has been widely reported as an effective additive to improve AD performance for accelerated biodegradation, increased methane production and enhanced process stability (Chen et al., 2014; Cruz Viggi et al., 2017; Shen et al., 2015b; Zhao et al., 2016a). One mechanism by which biochar improves AD performance is through promoting IET in methanogenic consortia, which highly depends on its electrochemical behavior (Cruz Viggi et al., 2017; Sun et al., 2017). Surface functional groups, such as quinone moieties, can reversibly donate and accept electrons, thus enables biochar to mediate microbial redox reactions in a similar manner to humic substances (Klüpfel et al., 2014b). Such a "battery" mechanism has been demonstrated to impact biogeochemical cycles of iron (Kappler et al., 2014; Xu et al., 2016) and nitrogen (Chen, G. et al., 2018a; Zhou et al., 2016), where redox-active biochars sustained electron transfer. Electron donating capacity (EDC) and electron accepting capacity (EAC) are commonly used parameters to characterize biochar's redox activity (Klüpfel et al., 2014a). In contrast, biochar formed at temperature >700 °C may function as an electrical conduit that allows direct electron transfer through carbon matrices, due to reduced number of redox-active functional groups and increased electrical conductivity (Sun et al., 2017). Similar to other conductive carbon materials (e.g. graphite, carbon cloth, granular activated carbon), conductive biochar may promote direct interspecies electron transfer (DIET) in syntrophic communities for enhanced methanogenesis (Chen et al., 2014; Zhao et al., 2016a).

However, it remains unknown about the role of electrochemical properties of biochar in methanogenic process, particularly during AD of complex organic waste stream like WAS, which involves different steps of biodegradation. To our best knowledge, this is the first study to comprehensively investigate the effect of biochar with distinct electrochemical properties on AD of WAS. The electrochemical properties of biochar usually depend on pyrolysis condition, especially the heating temperature (Klüpfel et al., 2014b). In this study, three types of biochars with distinctive electrochemical properties were prepared to investigate their impact on sludge AD process and microbial community. The main objective of this study is to elucidate the mechanism of increased methane production with biochar amendment in anaerobic digesters treating WAS. This study will strengthen the understanding of stimulatory mechanism of biochar in AD systems and contribute to proper biochar production as AD-stimulating additive.

2. Materials and methods

2.1. Biochar and sludge

Three types of biochars with distinctive electrochemical properties were produced by pyrolyzing corn stover biomass at different treatment temperatures. Prior to pyrolysis, biomass was grinded and sieved to obtain a particle size of 0.5 mm or less. Pyrolysis was carried out in a muffle furnace at atmospheric pressure and under oxygen-free condition, where ultrapure argon purge at 300 mL min^{-1} was used. Biomass was pyrolyzed at 300 °C, 500 °C and 700 °C, respectively, for 2 h to produce different types of biochars, designated as BC300, BC500 and BC700.

WAS as substrate used in the AD experiment was obtained from Minhang #2 municipal WWTP in Shanghai, China. Sludge was sieved through 1-mm mesh to discard coarse materials and stored at 4 °C until use. The inoculum was obtained from a mesophilic anaerobic digester treating municipal WAS, which has been continuously operated for over 2 years with stable performance. The main characteristics of the substrate sludge and inoculum were presented in the Supplementary Material (Table S1).

2.2. Characterization of biochars

2.2.1. Physicochemical properties

Morphology of biochar was characterized with a field-emission scanning electron microscopy (Sirion 200, FEI, USA). Brunauer-Emmett-Teller (BET) surface area was determined with an Autosorb-iQ instrument (Quantachrome, USA). Biochar pH was measured by mixing biochar powders in deionized water at solid/liquid ratio of 1:10 (w/v). Ash content was determined following the ASTM D3172-89 method and elemental contents were determined with an elemental analyzer (Vario Macro Cube, Elementar Analysensysteme, Germany). Surface functional groups were characterized by Fourier transform infrared spectroscopy (FTIR, Nicolet 6700, Thermo Scientific, USA) and X-ray photoelectron spectroscopy (XPS, ESCALAB 250XI, Thermo Scientific, USA). X-ray diffraction (XRD) patterns of carbon structure were acquired with a XRD-6100 Diffractometer (Shimadzu, Japan) using copper Kα radiation, with acquisition rate of 0.5° per min over a range of 10°−60°.

2.2.2. Electrochemical properties

The bulk electrical conductivity (EC) was measured with a four-point probe resistivity apparatus (ST2722, Suzhou Jingge, China). EAC and EDC of biochar were quantified according to a previous study (Klüpfel et al., 2014a). Electron exchange capacity (EEC) indicates the total capacity of biochar to accept and donate electrons (EEC = EAC + EDC).

2.3. Experiment of batch anaerobic digestion

Batch AD experiments were conducted in an AMPTS II system (Bioprocess Control, Sweden) according to the protocol of biochemical methane potential (BMP) tests (Angelidaki et al., 2009). The system has a total of 15 identical Schott glass bottles used as anaerobic digesters, each with a working volume of 400 mL. Four experimental groups were set up, including three test groups amended with different biochars (BC300, BC500 and BC700) and one control group (Control), each of which was operated in triplicate. For test groups, inoculum (80 mL) and substrate WAS (320 mL) were added in each bottle to acquire an initial total solids content of 3% for sludge biomass; biochar was added at dosage of 1.0 g/g dry weight of sludge. For control group, the ingredients were the same as the test groups, except that biochar was substituted with inert glass-fiber beads, which were ball-milled in advance to have an average diameter similar to the biochar. Before startup, each digester was degassed with high-purity helium for 5 min to obtain anaerobic condition. The temperature was maintained at 37 ± 1 °C and agitation speed was controlled at 60 rpm throughout the experiment. The gas outlet of each digester was connected to an airtight bottle containing 3 M NaOH solution for CO_2 sequestration. Subsequently, volume of CH_4 produced from each digester was measured and recorded by a real-time gas measurement unit. All the gas volume production data were reported at STP condition (273 K, 1 atm).

To further investigate the effect of biochar amendment on individual stages of WAS digestion, Test I and Test II batch experiments were carried out to assess the impact of biochar on hydrolysis-acidogenesis and acetogenesis-methanogenesis, respectively. The experimental setup for the two tests were almost the same as the above batch AD experiment with a few conditions changed, as described below.

Test I: The inoculum sludge was subjected to heat shock at 102 °C for 30 min to deactivate methanogens, while raw sludge was

used as the substrate (Oh et al., 2003). Chemical agent, 2-bromoethanesulfonate (BrES), was added at 50 mM to inhibit methanogenesis.

Test II: The raw WAS underwent alkaline fermentation for 8 days at 37 °C with pH maintained at 10.0 to facilitate VFAs production (Zhao et al., 2010). The resultant alkaline pretreated liquor (APL) contained a high concentration of VFAs and thus was used as the substrate for this batch of test. The pH of the APL was neutralized to 7.0 before used.

2.4. Kinetics analysis

A modified Gompertz model was employed to evaluate the kinetics of methane production (batch AD experiment and Test II), and a Logistic model was used to evaluate the kinetics of acidogenesis process for VFAs production (Test I). Detailed information of the model equations and parameters were described in the Supplementary Material.

2.5. Chemical analyses

Total solids (TS), volatile solids (VS), total chemical oxygen demand (TCOD) and total alkalinity were determined according to the standard methods (Baird et al., 2017). Liquid samples were centrifuged and filtered through 0.45 μm filters and the filtrate was characterized to obtain concentration of soluble COD (SCOD), soluble polysaccharides, soluble proteins and VFAs. Polysaccharides and proteins were determined with anthrone-sulfuric acid method and Coomassie Brilliant Blue method, respectively. VFAs were analyzed using a gas chromatography (7890, Agilent, USA) with a flame ionization detector. Biogas composition (CH_4 and CO_2) was analyzed using a gas chromatography (GC-2014, Shimadzu, Japan) with a thermal conductivity detector.

2.6. Microbial community analysis

To examine the microbial community composition, liquid digestate samples were collected on day 9 when the maximum methane production rate was achieved and on day 24 when the experiment was terminated in Test II. The samples were stored at −80 °C until further analysis. DNA extraction was performed using the FastDNA SPIN Kit (MP Biomedicals, Solon, OH) according to the manufacturer's instruction and the extracted DNA concentration was quantified with a NanoDrop 2000 UV−vis spectrophotometer (Thermo Scientific, Wilmington, DE). Subsequently, DNA samples were sent to Majorbio (Shanghai, China) for PCR amplification, sequencing and data processing and the detailed methods were described in the Supplementary Material.

2.7. Statistical analysis

Statistical analysis was performed using the "*vegan*" package in R (https://www.r-project.org/). One-way analysis of variance (ANOVA) was performed using the SPSS Statistics software (ver. 17.0).

3. Results and discussion

3.1. Performance of WAS anaerobic digestion amended with biochars

As shown in Fig. 1A, in comparison to the Control, biochar amendment increased the cumulative methane production by 46.9%, 28.9% and 11.2% for BC300 ($p < 0.001$), BC500 ($p < 0.001$) and BC700 ($p < 0.05$), respectively. Although biochar amendment

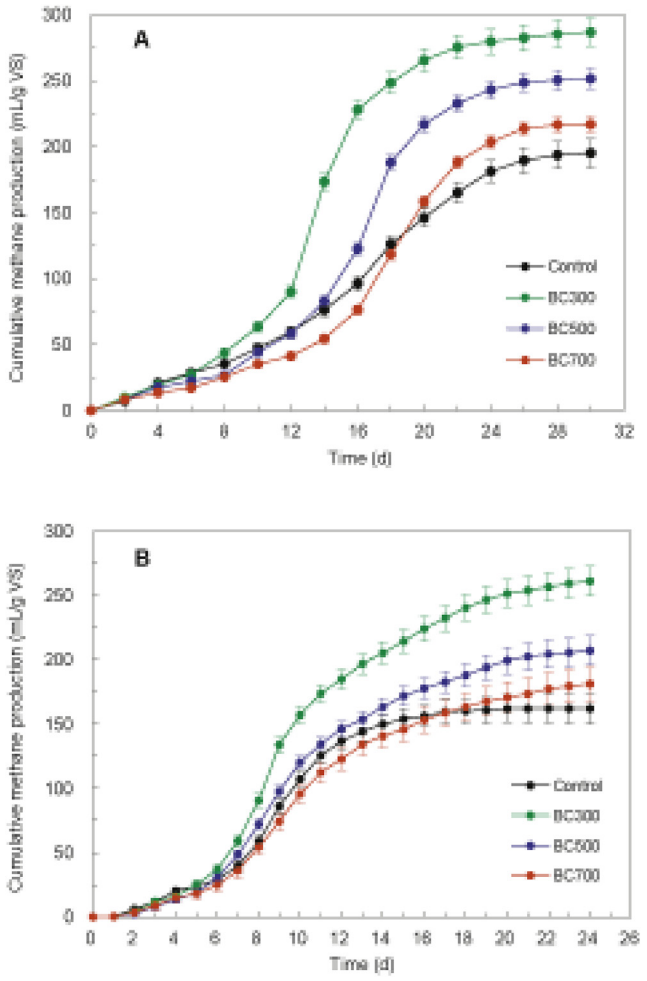

Fig. 1. Time-course profile of cumulative methane production during **(A)** single-stage batch AD experiment and **(B)** acetogenic-methanogenic stage in Test II. Data are presented as average values of biological replicates ($n = 3$), and error bars represent standard deviations.

prolonged the lag phase (λ), it remarkably increased the maximum methane production Rate(R_{max}) and the methane production potential (M_0) by up to 181.6% and 31.4%, respectively (Table 1). The prolonged lag phase by biochar addition could be attributed to the release of organic-binding metals (OBM, i.e. Ca, Mg, Al and Fe) from biochar during hydrolysis. The OBM has been demonstrated to significantly increase the activated energy for sludge hydrolysis (Xu et al., 2017). Overall, BC300 amendment resulted in the optimal performance of WAS anerobic digesters.

Test I and Test II were conducted individually to determine whether increased methane production by biochar amendment was mainly due to enhanced WAS hydrolysis-acidogenesis or acetogenesis-methanogenesis. During fermentation (Test I), soluble proteins and polysaccharides were generated from solubilization of

Table 1
Kinetics parameters describing the methane production process in the single-stage anaerobic digestion experiment, fitted with the modified Gompertz equation.

Group	λ (d)	R_{max} (mL·g^{-1} VS·d^{-1})	M_0(mL·g^{-1} VS)	R^2
Control	5.21 ± 0.04	9.65 ± 2.09	200.68 ± 10.45	0.992
BC300	7.61 ± 0.14	27.17 ± 3.14	263.67 ± 8.89	0.985
BC500	8.82 ± 0.12	19.61 ± 3.23	223.59 ± 17.24	0.980
BC700	9.35 ± 0.09	14.77 ± 1.35	208.18 ± 19.34	0.981

particulate organics and subsequently degraded by acidogenic bacteria for production of VFAs (Supplementary Material, Fig. S1). Acetate was the predominant VFA, followed by propionate, *iso*-butyrate, *iso*-valerate, *n*-butyrate and *n*-valerate (Supplementary Material, Fig. S2). By the end of fermentation, BC300, BC500 and BC700 increased the SCOD concentration by 9.5%, 3.8% and 9.4%, respectively, and increased the total VFAs concentration by 12.3%, 3.2% and 9.4%, respectively. However, none of the above increase in SCOD or total VFAs production was statistically significant as compared to the Control ($p > 0.05$). Moreover, similar kinetics parameters were obtained for VFAs production, with no significant difference between the biochar-amended digesters and Control ($p > 0.05$) (Table 2). The above results demonstrated that adding biochar, irrespective of the electrochemical properties, did not promote WAS hydrolysis or acidogenesis prior to methanogenesis. This could be attributed to the limited interaction between biochar and sludge flocs or hydrolytic enzymes regulated by electrostatic force, covalent bonds and sweep flocculation (Li et al., 2019).

For Test II, VFA-enriched sludge APL was used as the substrate. Acetate and propionate were the two major VFAs in the APL. The biochar-amended digesters achieved a significant increase in the cumulative methane production by 61.0%, 27.8% and 11.8% for BC300 ($p < 0.001$), BC500 ($p < 0.001$) and BC700 ($p < 0.01$), respectively, as compared to the Control (Fig. 1B). No significant difference ($p > 0.05$) was observed in the lag phase (λ) among the digester groups (Table 3). However, BC300, BC500 and BC700 increased the methane production potential (M_0) substantially by 78.4%, 22.3% and 12.9%, respectively. BC300 significantly increased the maximum methane production rate (R_{max}) by 34.1% ($p < 0.001$), while BC500 and BC700 decreased the R_{max} by 24.7% ($p < 0.01$) and 31.4% ($p < 0.01$), respectively. Taken together, the methanogenic performance of digesters in Test II was ranked as BC300 > BC500 > BC700 > Control, showing a similar pattern as observed in the single-stage batch AD experiment (Fig. 1A). Methane formation generally corresponds with VFAs degradation. Rapid degradation of VFAs was observed before day 12 (Fig. 2). Afterwards, the rate of VFAs degradation sharply decreased and their concentration almost remained unchanged towards the end. Notably, BC300 substantially accelerated degradation of acetate, propionate and *iso*-valerate (Fig. 2A, B, 2F). Degradation of C_4 fatty acids showed a similar pattern across the test groups (Fig. 2C and D), while BC500 accelerated degradation of C_5 fatty acids (Fig. 2E and F). The results of Test I and II indicated that the stimulatory impact of biochar on methane production was more associated with the acetogenic-methanogenic stages rather than the prior steps during AD of WAS.

3.2. Physicochemical and electrochemical properties of biochars

Table 4 summarized the physical and chemical properties of the biochars prepared at different pyrolysis temperatures. The BET surface area (19.8–32.8 m^2/g) was comparable to those of corn stover biochars prepared under similar charring conditions (Brewer et al., 2009; Lee et al., 2010). SEM images showed that both BC300 and BC500 had rough surface with pores randomly aligned, whereas BC700 was noticeably porous (Supplementary Material, Fig. S3). The biochars contained moderate amount of ash (15.9–22.1 DW%), mainly due to the relatively high ash content in the corn stover feedstock (Brewer et al., 2009). The hydrogen (H) and oxygen (O) content in biochars decreased with the increase of pyrolysis temperature, while the carbon (C) content showed a reverse trend. As a result, BC700 had the lowest H:C (0.28) and O:C (0.06) molar ratios, suggesting a high degree of aromatic condensation.

FTIR spectra showed that various surface functional groups were obtained at different pyrolysis temperatures (Fig. 3A). For BC300 and BC500, the broad peaks between 1580 cm^{-1} and 1700 cm^{-1} corresponded to stretching of C=C and C=O bonds, indicating formation of aromatic carbon, ketones and carboxyl groups. The band at 1400 cm^{-1} could be due to both O–H in-plane bending and C–H bending. Various bands in the spectrum corresponded to lone aryl C–H wag (846 cm^{-1}) and two-adjacent aryl C–H wags (790 cm^{-1}), and the band at 3000 cm^{-1} represented the symmetric CH_3 stretch of the methoxyl group (partially caused by O–H stretching). The bands of above 3500 cm^{-1} are due to alcoholic or phenolic components. In contrast, no featured vibrations were observed for BC700, indicating reduced amount of redox-active groups. In addition, XPS analytical results provided complementary information of biochar's surface properties (Supplementary Material, Fig. S4). The C1s spectra showed presence of C–C/C=C, C–O, C=O and O=C–O groups in the biochar. With the pyrolysis temperature increased, the peak intensities of C–C/C=C groups increased, while the intensities of oxygen groups decreased, suggesting less distribution of C–O/C=O/O=C–O groups in the inner sheets.

All the biochar samples showed amorphous structures in contrast to the crystalline graphite reference (Fig. 3B). The XRD spectra showed broad peaks at 23° and 43°, corresponding to the (002) peak and (10) peak of the turbostratic domains in carbon structure, respectively (Keiluweit et al., 2010). The average perpendicular height of the turbostratic domains (L_c) and the average in-plane width of graphene nanosheets (L_a) were employed to examine the carbon structure. The interlayer spacing $d_{(002)}$ (3.79–3.96 Å) for the biochars was much larger than that for crystalline graphite (3.35 Å) (Supplementary Material, Table S2). With pyrolysis temperature increased from 300 °C to 700 °C, the L_c of biochar only increased slightly from 0.95 nm to 1.15 nm, while the L_a substantially increased from 1.06 nm to 3.74 nm (Fig. 3C). The larger in-plane crystalline size of BC700 indicates reduced electrical resistivity (Sun et al., 2018), which was also reflected in an increase in biochar's EC as discussed below.

The EC of biochar increased with the increase in pyrolysis temperature (Fig. 3D). BC300 was nearly not conductive with EC of 8×10^{-9} S/m, while EC of BC500 and BC700 increased to 7×10^{-5} S/m and 101.3 S/m, respectively. Such an increase in EC is generally derived from formation of graphene-like structure in biochar with conjugated π-electron systems that facilitate direct electron transfer through carbon matrix (Xu et al., 2013). The EDC of biochar decreased with pyrolysis temperature, while the EAC showed an

Table 2
Kinetics parameters describing the VFAs production process in the staged anaerobic digestion experiment (hydrolysis-acidogenesis), fitted with the Logistic model.

Group	k_{VFA} (d^{-1})	C_{max} (mg COD·L^{-1})	C_0 (mg COD·L^{-1})	R^2
Control	1.53 ± 0.09	3541.3 ± 47.5	555.3 ± 49.3	0.970
BC300	1.72 ± 0.59	3888.4 ± 102.2	587.2 ± 44.2	0.958
BC500	1.93 ± 0.51	3402.6 ± 52.2	548.1 ± 61.6	0.999
BC700	1.69 ± 0.69	3914.5 ± 72.1	569.2 ± 40.2	0.975

Table 3
Kinetics parameters describing the methane production process in the staged anaerobic digestion experiment (acetogenesis-methanogenesis), fitted with the modified Gompertz equation.

Group	λ (d)	R_{max} (mL·g^{-1} VS·d^{-1})	M_0 (mL·g^{-1} VS)	R^2
Control	3.69 ± 0.05	16.74 ± 1.01	126.69 ± 5.99	0.994
BC300	3.50 ± 0.02	22.45 ± 3.01	225.97 ± 1.11	0.982
BC500	3.47 ± 0.04	12.60 ± 1.53	154.96 ± 19.96	0.991
BC700	3.68 ± 0.02	11.48 ± 2.22	143.07 ± 15.40	0.992

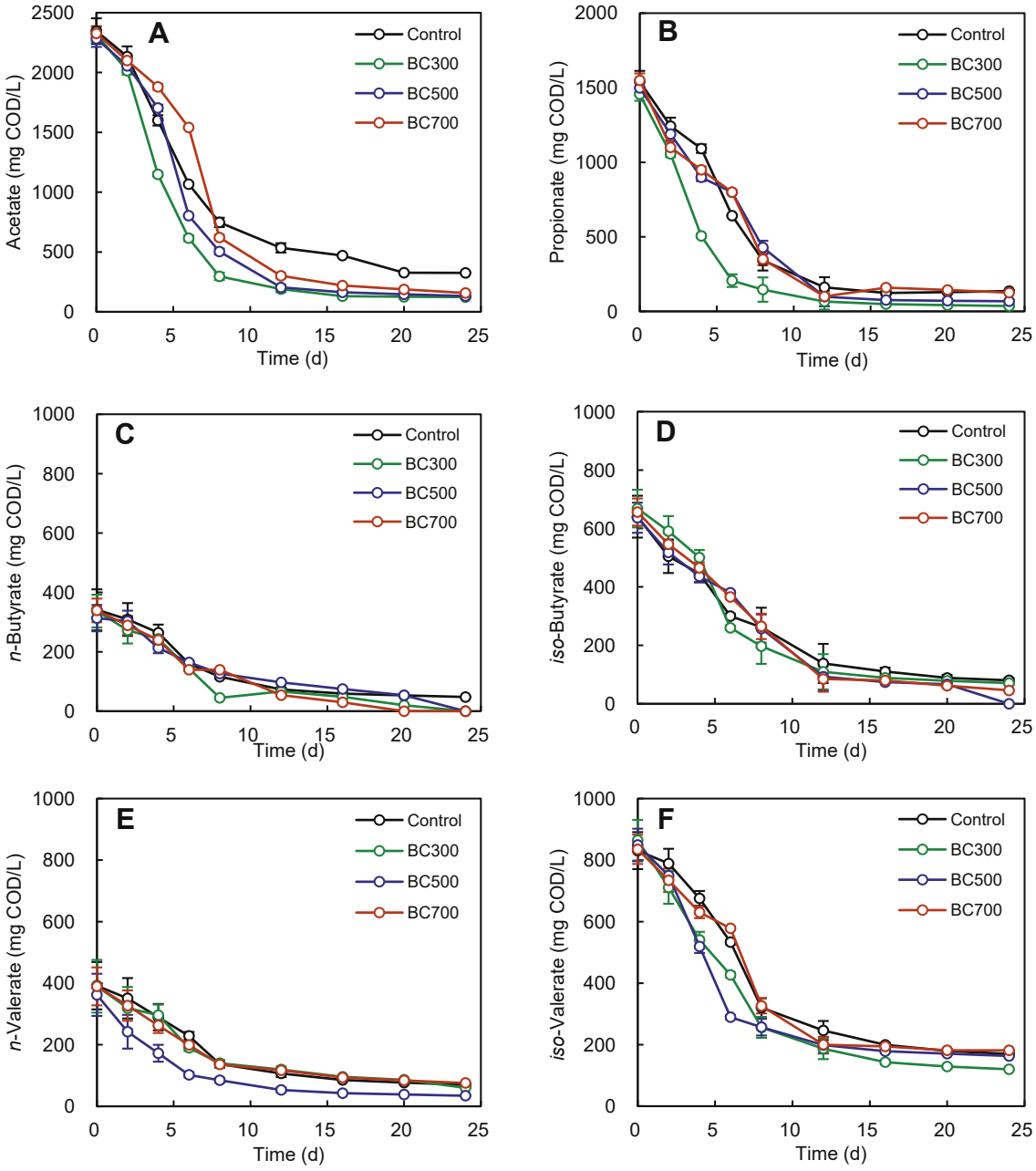

Fig. 2. Effect of different biochars on methanogenesis stage of WAS anaerobic digestion: time-course profiles of **(A)** acetate, **(B)** propionate, **(C)** *n*-butyrate, **(D)** *iso*-butyrate, **(E)** *n*-valerate and **(F)** *iso*-valerate. Data are presented as average values of biological replicates ($n = 3$), and error bars represent standard deviations.

opposite trend (Fig. 3E). BC300 had the highest EDC (0.598 mmol e^-/g), whereas BC700 had the lowest EDC (0.228 mmol e^-/g) but the highest EAC (0.740 mmol e^-/g). The decrease in EDC was attributed to the reduced amount of redox-active functional groups such as hydroquinone-quinone pairs (Cruz Viggi et al., 2017; Klüpfel et al., 2014a). The trends in EDC and EAC resulted in the EEC value of BC300 (1.007 mmol e^-/g) similar to that of BC700 (0.968 mmol e^-/g), whereas BC500 had the lowest EEC (0.626 mmol e^-/g).

3.3. Correlating the methanogenic performance of WAS anaerobic digestion to the electrochemical properties of biochar

The results of Test II showed that biochars with distinctive electrochemical properties promoted the methanogenic performance of WAS digestion to varying extents. To better understand the role of

Table 4
Physicochemical characteristics of biochars [a].

Parameter	BC300	BC500	BC700
BET surface area (m^2/g)	19.75 ± 0.72	20.05 ± 1.52	32.76 ± 2.01
Total pore volume (cm^3/g)	0.02 ± 0.00	0.02 ± 0.00	0.04 ± 0.01
Particle size (d_{50}, μm)	310 ± 10	301 ± 7	309 ± 8
pH	8.35 ± 0.06	10.12 ± 0.8	10.39 ± 1.24
Ash (DW%) [b]	15.87 ± 1.14	20.43 ± 2.05	22.06 ± 6.11
C (DW%)	61.10 ± 5.05	64.78 ± 3.11	72.88 ± 2.34
H (DW%)	3.88 ± 0.61	2.49 ± 0.11	1.70 ± 0.51
O (DW%)	17.49 ± 1.88	10.89 ± 0.26	2.44 ± 0.04
N (DW%)	1.41 ± 0.01	1.22 ± 0.00	0.73 ± 0.05
S (DW%)	0.25 ± 0.01	0.19 ± 0.00	0.19 ± 0.01
H:C molar ratio	0.76 ± 0.01	0.46 ± 0.00	0.28 ± 0.00
O:C molar ratio	0.21 ± 0.02	0.13 ± 0.00	0.06 ± 0.00

[a] Data are presented as average values of biological replicates ($n = 3$) ± standard deviations.
[b] DW: dry weight.

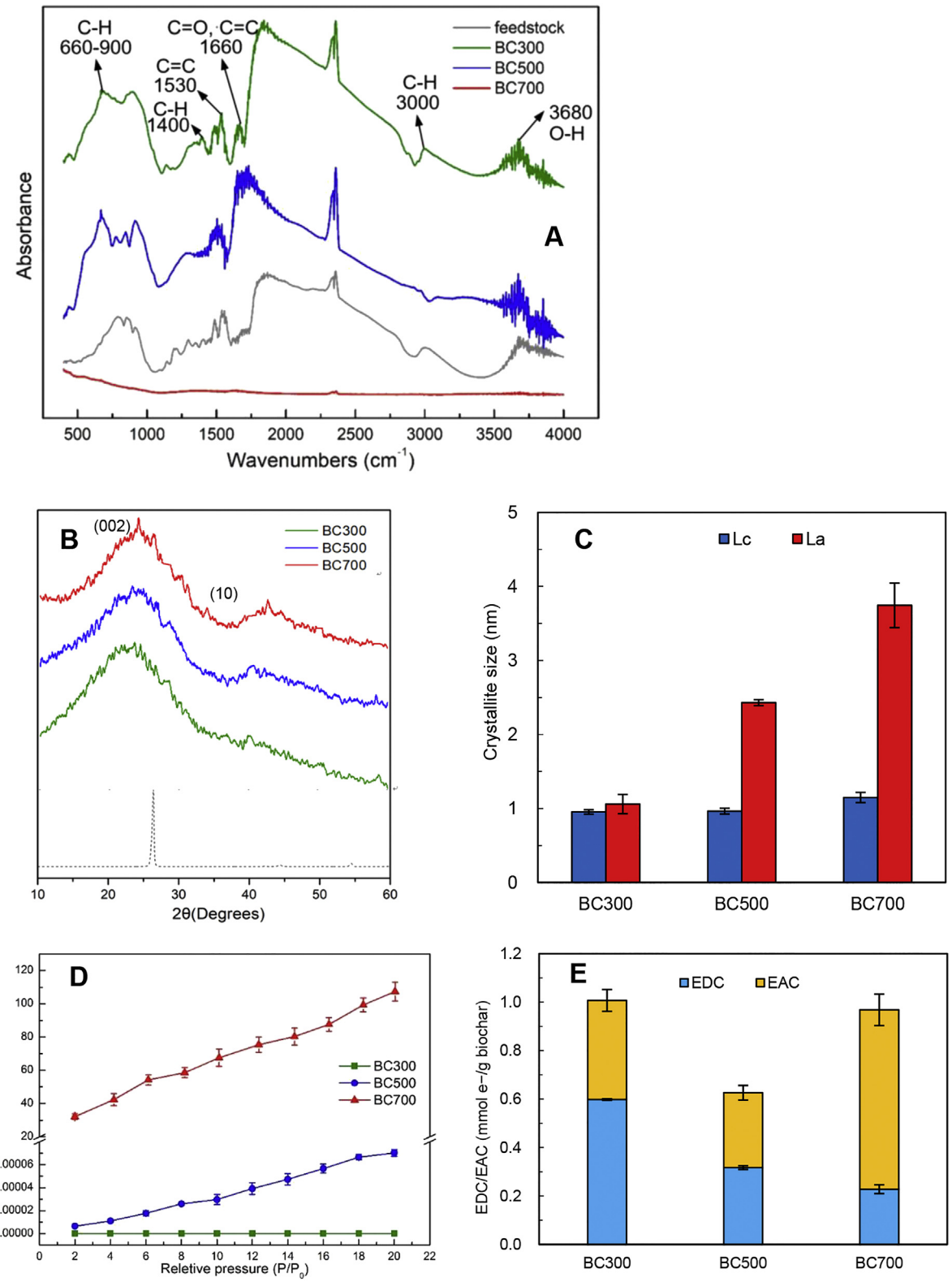

Fig. 3. Characterization of biochars. **(A)** FTIR spectra; **(B)** X-ray diffraction patterns; the dashed line represents the spectrum of graphite as a reference; **(C)** dimensions of turbostratic domains, where L_c and L_a represent the average perpendicular height of the turbostratic domains and the average in-plane width of graphene nanosheets, respectively; **(D)** bulk electrical conductivity; **(E)** electron donating capacity (EDC) and electron accepting capacity (EAC). Error bars represent standard deviations of triplicate measurements.

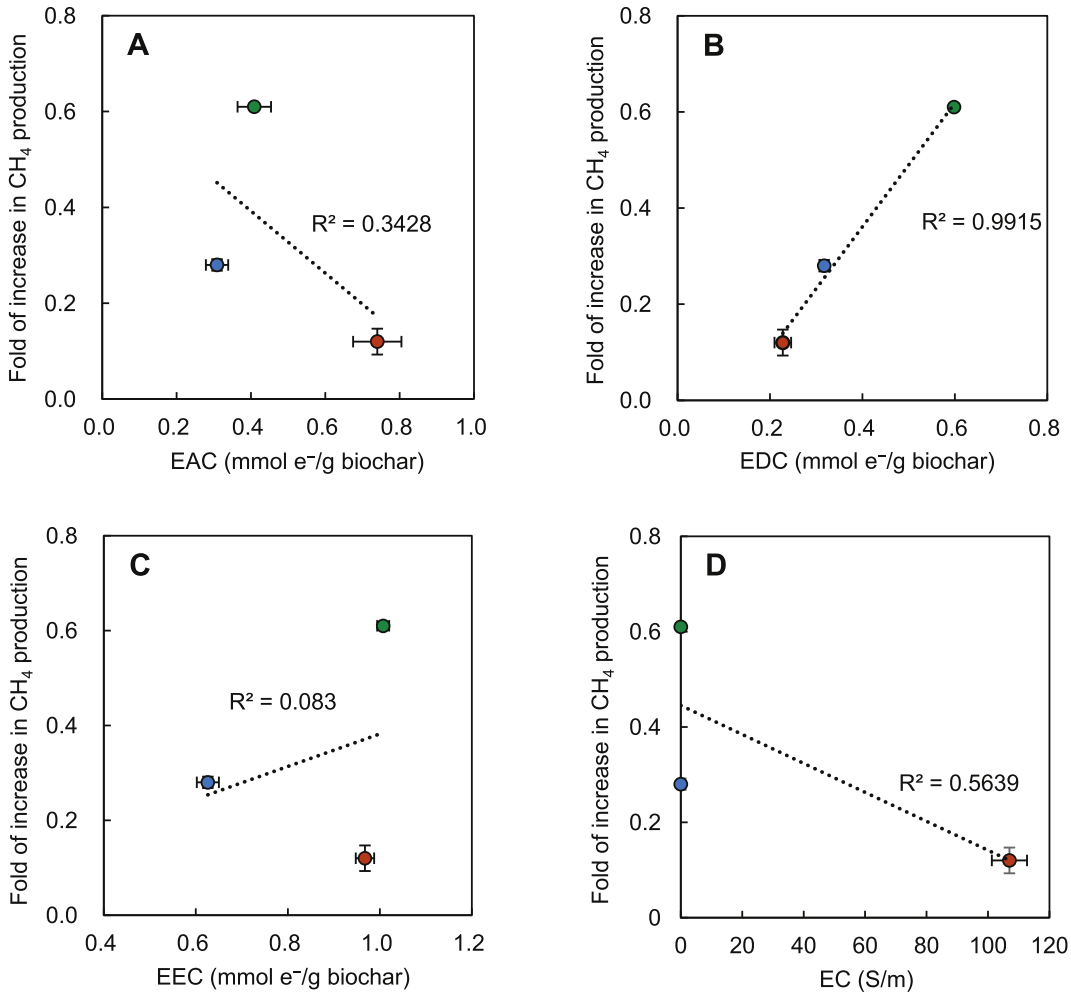

Fig. 4. Correlation between the fold of increase in methane production from digesters amended with biochars during staged anaerobic digestion experiment (methanogenesis) as compared to the Control digester and the electrochemical properties of biochar, including **(A)** electron accepting capacity (EAC), **(B)** electron donating capacity (EDC), **(C)** electron exchange capacity (EEC) and **(D)** electrical conductivity (EC). Legends: green (BC300), blue (BC500) and red (BC700). Error bars represent standard deviations of biological triplicates (methane production) or triplicate measurements (biochar electrochemical properties). (For interpretation of the references to color in this figure legend, the reader is referred to the Web version of this article.)

biochar's electrochemical properties, we correlated the methanogenic performance to the biochar's EDC, EAC, EEC and EC, respectively (Fig. 4). Specifically, the methanogenic performance of the biochar-amended digesters was quantified as the fold of increase in volumetric methane production as compared to the Control digester (CH_4-fold). A positive linear correlation ($R^2 = 0.992$) was noted between the CH_4-fold and biochar's EDC (Fig. 4B). However, it was not the case for biochar's EAC (Fig. 4A), EEC (Fig. 4C) or EC (Fig. 4D). The results indicated that the redox-active functional groups, particularly electron-donating hydroquinone moieties, could play a crucial role in facilitating methanogenesis. Such an electrochemical behavior promotes electron transfer through charging-discharging cycles, which is different from the direct electron transfer through the carbon matrix. The former makes biochar function as a rechargeable battery, whereas the latter is induced by bulk electrical conductivity (Sun et al., 2017). Surprisingly, amending WAS digester with the most conductive biochar (BC700) did not lead to the largest increase in methane production, as reflected in the weak negative correlation ($R^2 = 0.564$) between the CH_4-fold and biochar's EC (Fig. 4D). Despite that the EC of BC300 was 12.7 billion times lower than that of BC700, BC300 digesters had superior AD performance, with remarkably higher methane production (by 32.1%) and higher maximum methane production rate (by 84.0%). The above findings suggest that biochar may improve methane production, at least for AD of WAS, independently of its bulk conductivity, which was consistent with the recent studies on biochar-promoted methanogenesis obtained in ethanol-metabolizing *Geobacter* co-cultures (Chen et al., 2014; Yuan et al., 2018) and food waste-degrading consortia (Cruz Viggi et al., 2017).

3.4. Microbial community composition and dynamics in the digesters

An average of 1084 and 43 OTUs were obtained per sample for bacteria and archaea, respectively (Supplementary Material, Table S3 and S4). For bacteria, *Firmicutes*, *Bacteroidetes* and *Proteobacteria* were the dominant communities at the phylum level, with relative abundance of 41.7–54.6%, 14.6–22.4% and 12.8–23.8%, respectively. At the class level, *Clostridia*, *Bacteroidia*, *Bacilli* and *Gammaproteobacteria* were the most abundant bacterial communities (Fig. 5A). The relative abundance of *Clostridia* increased from day 9 to day 24, while those of *Bacteroidia* and *Bacilli* decreased in all the digesters. On average, the relative abundance of *Clostridia* was 37.1%, 34.0% and 35.8% in BC300, BC500 and BC700,

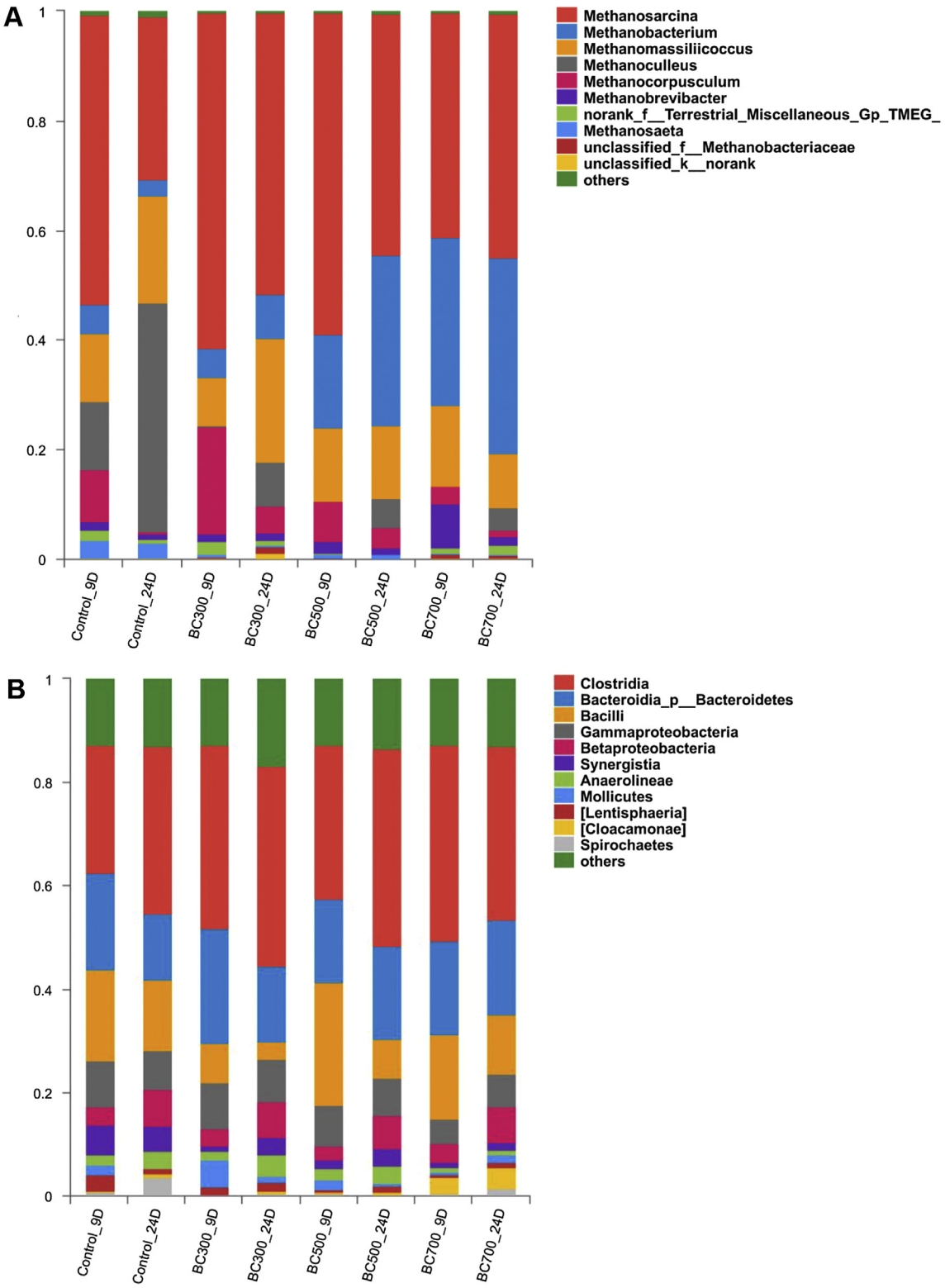

Fig. 5. Microbial community composition of the most abundant taxa in the digester culture based on 16S rRNA gene sequencing data: **(A)** bacteria at the class level and **(B)** archaea at the genus level. The relative abundance is calculated as the percentage of the targeted sequence to the total high-quality sequences of each sample.

respectively, which was significantly ($p < 0.01$) higher than that in the Control (28.5%), indicating that biochar addition could enrich *Clostridia*. In general, no remarkable difference was observed in the bacterial communities composition between the Control and biochar-amended digesters.

Both hydrogenotrophic and acetoclastic methanogens were found in the digesters, but hydrogenotrophic methanogens dominated the archaeal communities (Fig. 5B). At the genus level, *Methanosarcina* was the most abundant methanogen, with relative abundance of 47.9%, averaged over all the samples. *Methanobacterium* was present

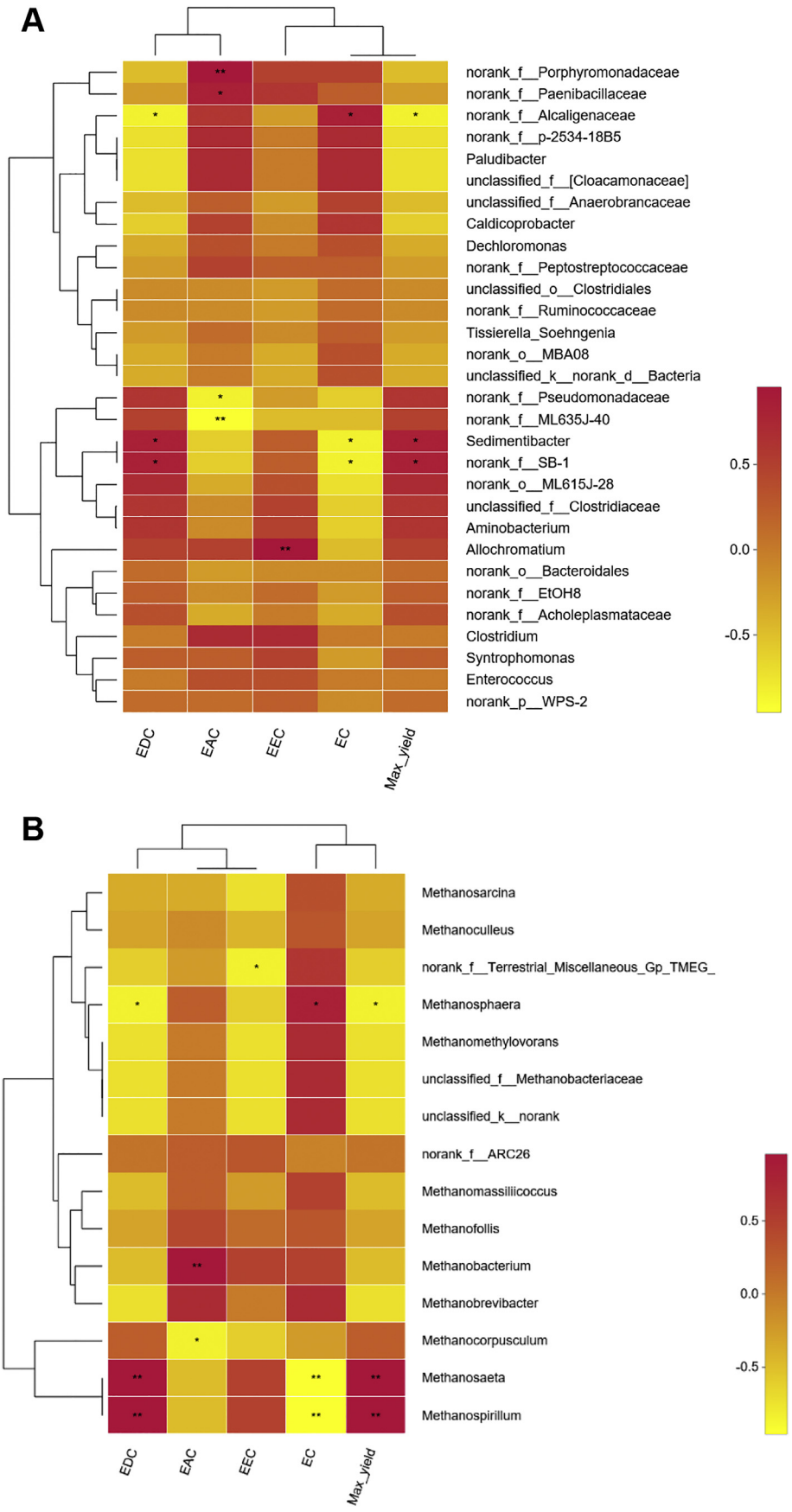

Fig. 6. Spearman correlation heatmap showing relative abundance of microbial communities at the genus level in response to electrochemical properties of biochar amended in the digesters and methane production: **(A)** bacterial community **(B)** archaeal community. The color gradient indicates Spearman's rank correlation coefficient (ρ) with more positive

in the Control and BC300, but their relative abundance was substantially higher in BC500 (24.0%) and BC700 (33.3%). The relative abundance of *Methanoculleus* increased from 12.3%, 0.2%, 0.1% and 0.1% on day 9—41.6%, 8.2%, 5.2% and 4.2% on day 24 in the Control, BC300, BC500 and BC700, respectively. In contrast, the relative abundance of *Methanocorpusculum* decreased from 9.5%, 19.6%, 7.2% and 3.1% on day 9 to 0.4%, 4.8%, 3.9% and 1.1% on day 24 in the Control, BC300, BC500 and BC700, respectively. Noticeably, acetoclastic *Methanosaeta* showed a much higher relative abundance in the Control (2.9%) as compared to the biochar-amended digesters (average 0.4%). Additionally, the obligately H_2-dependent methylotrophic *Methanomassiliicoccales* was present as one of the most predominant methanogens in all the digestate samples, with the relative abundance ranging from 8.9% to 22.6%. Overall, the archaeal community profiles suggest that methane was predominantly produced through hydrogenotrophic methanogenesis.

Significant correlations ($p < 0.05$) were observed between the redox activity-associated parameters (i.e. EDC, EAC and EEC) and a few bacterial taxa. Fig. 6A showed a significant positive correlation ($p < 0.05$) between the biochar's EDC and abundance of amino acid-utilizing *Sedimentibacter*, very significant positive correlation ($p < 0.01$) between the biochar's EAC and abundance of acidogenic *Porphyromonadaceae*, a very significant positive correlation ($p < 0.01$) between the biochar's EEC and abundance of sulfur bacterium *Allochromatium*, a significant negative correlation ($p < 0.05$) between the biochar's EDC and abundance of sulfate-reducing *Alcaligenaceae* and a very significant negative correlation ($p < 0.01$) between the biochar's EAC and abundance of alkalophilic and halotolerant *Bacteroidaceae* "ML635J-40". For archaeal communities, analysis revealed a very significant positive correlation ($p < 0.01$) between the biochar's EDC and abundance of acetoclastic *Methanosaeta* and hydrogenotrophic *Methanospirillum* (Evans et al., 2019), a significant negative correlation ($p < 0.05$) between the biochar's EDC and H_2-dependent methylotrophic *Methanosphaera* and a very significant negative correlation ($p < 0.01$) between the biochar's EAC and abundance of hydrogenotrophic *Methanobacterium* (Fig. 6B). These results revealed the importance of biochar's electrochemical functions to the overall methane production. The correlations of *Alcaligenaceae*, *Sedimentibacter* and unclassified *Bacteroidetes* family "SB-1" abundance to the methane yield were consistent with those to the EDC, but were contrary to those to the EC. Likewise, the correlations of *Methanosaeta*, *Methanospirillum* and *Methanosphaera* abundance to the methane yield were consistent with those to the EDC, but were converse to those to the EC. Interestingly, no significant correlation was observed between the abundance of *Methanosarcina* and electrochemical properties of biochar.

3.5. Underlying mechanism of biochar amendment to promote methanogenic performance of anaerobic digesters treating WAS

Biochar can facilitate electron transfer by surface functional groups and/or inner carbon matrices. Biochar derived from low-temperature pyrolysis is generally enriched with functional groups that can donate and accept electrons to promote microbial redox reactions (Sun et al., 2017). Herein, the fastest degradation of propionate by BC300 (Fig. 2B) indicated the facilitated syntrophy between propionate-oxidizing acetogens and hydrogenotrophic methanogens with accelerated IET, thus substantially improving the methane production. Recently Sun et al. (2017) showed that the extent of functional groups or carbon matrices contributing to electron transfer is significantly related to biochar's H:C and O:C molar ratios. For biochar with H:C and O:C molar ratios of 0.35—0.62 and 0.09—0.24, electron transfer is predominantly mediated by redox-active functional groups. For biochar with H:C < 0.19 and O:C < 0.06, more ordered graphitic structures forming at high pyrolysis temperature (>700 °C) establish a shortcut pathway for direct electron transfer. Provided that the threshold H:C and O:C molar ratios observed for the transition can be extrapolated to this study, BC300 (H:C = 0.76, O:C = 0.21) and BC500 (H:C = 0.46, O:C = 0.13) mediate the electron transfer in syntrophic communities through redox cycles of functional groups, while BC700 (H:C = 0.28, O:C = 0.06) functions like an electric conduit. Theoretically, EEC is the parameter that determines the capacity of biochar to mediate redox reactions. However, despite the comparable EEC values observed in BC300 and BC700 (Fig. 3C), the considerable difference in methane production (Fig. 1B) suggests that EDC plays a more important role than EAC or EEC. High-EDC biochar would increase the number of electrons transported to methanogens, supporting methanogenesis via CO_2 reduction. This phenomenon was also observed in other biological processes, where biochar formed at mild pyrolysis temperature (250—500 °C) facilitates denitrification (Chen, G. et al., 2018), dissimilatory Fe(III) reduction (Xu et al., 2016) and reduction of toxic pollutants (Chen, J. et al., 2018). The highly efficient degradation of acetate (Fig. 2A) and propionate (Fig. 2B) in the BC300-amended digester tends to support this proposed theory, because syntrophic acetate or propionate oxidation must couple to hydrogenotrophic methanogenesis. Moreover, some hydrogenotrophic methanogens are capable of direct uptake of electrons (Lohner et al., 2014). Biochar-induced electrons might also promote methanogenesis via this route. In contrast, high-EAC biochar may become an electron sink, which would competitively reduce electrons transferred to CO_2 and inhibit methanogenesis (Klüpfel et al., 2014).

As a porous material, biochar provides supporting surface for microbes to attach on. For example, biochar selectively enriched *Methanosaeta* and *Methanosarcina* against stress of acids and ammonium (Lü et al., 2016; Luo et al., 2015). In contrast, biochars used in this study were unable to enrich *Methanosaeta*. Their abundance was significantly lower ($p < 0.001$) in the biochar-amended digesters than the control. These obligate acetoclastic methanogens had very low abundance across the test groups, suggesting that syntrophic acetate oxidation was the primary pathway (Karakashev et al., 2006). However, the relative abundance of *Methanosarcina* was only slightly higher in the biochar-amended digesters than that in the control. On the other hand, hydrogenotrophic *Methanobacterium* genera were highly enriched in the presence of biochar, particularly BC500 and BC700. When syntrophic microbial communities attach to biochar surface, the syntrophic partners are generally in closer physical association. This may compensate the long-range IET mediated by H_2 for dispersed cells. However, more experimental evidence will be needed to demonstrate to what extent microbial attachment could promote methanogenesis.

DIET is suggested as a possible mechanism of the enhanced methanogenesis by biochar amendment (Chen et al., 2014; Zhao et al., 2016a). As an alternative mode of IET in AD, DIET occurs through microbial e-pili or conductive materials (Lovley, 2017; Rotaru, A.-E. et al., 2014a). However, despite the greatest increase in methane production, BC300 is not conductive. Conversely,

values (red) indicating stronger positive correlations and more negative values (yellow) indicating stronger negative correlations. The number of asterisks denote the statistical significance levels (two-tailed) of the Spearman's ρ value, *$p < 0.05$, **$p < 0.01$ and ***$p < 0.001$. (For interpretation of the references to color in this figure legend, the reader is referred to the Web version of this article.)

conductive BC700 might facilitate DIET, but it did not result in the best improvement in AD performance. Therefore, it is arguable that DIET is the dominant mechanism for enhanced methanogenic performance with biochar amendment, at least not in the case of sludge digesters. So far, only defined co-cultures of *Geobacter metallireducens* and two methanogenic archaea (*Methanothrix harundinacea* and *Methanosarcina barkeri*) are conclusively proven to perform DIET (Rotaru, A.-E. et al., 2014b; Rotaru, A.E. et al., 2014a). Although DIET is widely suggested as the mechanism of syntrophic electron transport involved in methanogenic consortia with conductive carbon materials, DIET has been postulated merely based on the fact that microorganisms known to perform DIET (e.g. *Geobacter* species) were identified or enriched (Dang et al., 2016; Zhao, Z. et al., 2017b; Zhao et al., 2016a; Zhao, Zhiqiang et al., 2017a; Zhao et al., 2016b). However, in this study, none of the aforementioned DIET-microbes were enriched in the biochar-amended digesters. On the other hand, recent studies based on meta-omics approaches revealed that *Syntrophomonas*, *Thauera*, *Methanospirillum* and *Methanosphaerula* may participate in DIET (Dang et al., 2016; Jing et al., 2017; Wang et al., 2018), further research will be needed to provide more straightforward experimental evidence to determine the contribution of biochar's electrochemical properties to DIET and if promoting DIET will improve the performance of digesters treating complex organic waste like WAS.

4. Conclusions

In summary, this work compares the methanogenic performance of anaerobic digesters amended with biochars prepared at different pyrolysis temperatures. The results show that the stimulatory effect of biochar on methane production during AD of WAS is more associated with the acetogenic-methanogenic stages and that the ability of biochar for enhanced methanogenesis highly depends on its redox activity, especially EDC, rather than its conductivity. Electron transfer mediated by the redox-active groups may perform as a dominant mechanism for the stimulatory effect of biochar on methanogenesis. Future studies will be needed to kinetically and quantitively investigate the importance of biochar's redox cycle to IET in syntrophic communities and also to determine if such a "battery mechanism" is sustainable so that redox-active biochar can have a long-term impact on the methanogenic performance of WAS digesters for practical applications.

CRediT authorship contribution statement

Yanwen Shen: Conceptualization, Methodology, Writing - review & editing. **Yamei Yu:** Investigation, Writing - original draft. **Yue Zhang:** Methodology, Visualization. **Meltem Urgun-Demirtas:** Supervision. **Haiping Yuan:** Validation. **Nanwen Zhu:** Supervision. **Xiaohu Dai:** Supervision.

Declaration of competing interest

The authors declare that they have no known competing financial interests or personal relationships that could have appeared to influence the work reported in this paper.

Acknowledgements

This work was supported by Shanghai Pujiang Program (18PJ1406300), Program for Professor of Special Appointment (Eastern Scholar) at Shanghai Institutions of Higher Learning (2017) and National Natural Science Foundation of China (21876110).

Appendix A. Supplementary data

Supplementary data to this article can be found online at https://doi.org/10.1016/j.jclepro.2020.123212.

References

Angelidaki, I., Alves, M., Bolzonella, D., Borzacconi, L., Campos, J.L., Guwy, A.J., Kalyuzhnyi, S., Jenicek, P., van Lier, J.B., 2009. Defining the biomethane potential (BMP) of solid organic wastes and energy crops: a proposed protocol for batch assays. Water Sci. Technol. 59 (5), 927–934.

Angenent, L.T., Usack, J.G., Xu, J., Hafenbradl, D., Posmanik, R., Tester, J.W., 2018. Integrating electrochemical, biological, physical, and thermochemical process units to expand the applicability of anaerobic digestion. Bioresour. Technol. 247, 1085–1094.

Baird, R.B., Eaton, A.D., Rice, E.W., 2017. Standard Methods for the Examination of Water and Wastewater, 23rd Edition. American Public Health Association (APHA), American Water Works Association (AWWA), Water Environment Federation (WEF), United States.

Brewer, C.E., Schmidt-Rohr, K., Satrio, J.A., Brown, R.C., 2009. Characterization of biochar from fast pyrolysis and gasification systems. Environ. Prog. Sustain. Energy 28 (3), 386–396.

Chen, G., Zhang, Z., Zhang, Z., Zhang, R., 2018a. Redox-active reactions in denitrification provided by biochars pyrolyzed at different temperatures. Sci. Total Environ. 615, 1547–1556.

Chen, J., Wang, C., Pan, Y., Farzana, S.S., Tam, N.F., 2018b. Biochar accelerates microbial reductive debromination of 2,2',4,4'-tetrabromodiphenyl ether (BDE-47) in anaerobic mangrove sediments. J. Hazard Mater. 341, 177–186.

Chen, S., Rotaru, A.E., Shrestha, P.M., Malvankar, N.S., Liu, F., Fan, W., Nevin, K.P., Lovley, D.R., 2014. Promoting interspecies electron transfer with biochar. Sci. Rep. 4, 5019.

Cruz Viggi, C., Simonetti, S., Palma, E., Pagliaccia, P., Braguglia, C., Fazi, S., Baronti, S., Navarra, M.A., Pettiti, I., Koch, C., Harnisch, F., Aulenta, F., 2017. Enhancing methane production from food waste fermentate using biochar: the added value of electrochemical testing in pre-selecting the most effective type of biochar. Biotechnol. Biofuels 10, 303.

Dang, Y., Holmes, D.E., Zhao, Z., Woodard, T.L., Zhang, Y., Sun, D., Wang, L.Y., Nevin, K.P., Lovley, D.R., 2016. Enhancing anaerobic digestion of complex organic waste with carbon-based conductive materials. Bioresour. Technol. 220, 516–522.

Evans, P.N., Boyd, J.A., Leu, A.O., Woodcroft, B.J., Parks, D.H., Hugenholtz, P., Tyson, G.W., 2019. An evolving view of methane metabolism in the Archaea. Nat. Rev. Microbiol. 17 (4), 219–232.

Heidrich, E.S., Curtis, T.P., Dolfing, J., 2011. Determination of the internal chemical energy of wastewater. Environ. Sci. Technol. 45 (2), 827–832.

Jing, Y., Wan, J., Angelidaki, I., Zhang, S., Luo, G., 2017. iTRAQ quantitative proteomic analysis reveals the pathways for methanation of propionate facilitated by magnetite. Water Res. 108, 212–221.

Kappler, A., Wuestner, M.L., Ruecker, A., Harter, J., Halama, M., Behrens, S., 2014. Biochar as an electron shuttle between bacteria and Fe(III) minerals. Environ. Sci. Technol. Lett. 1 (8), 339–344.

Karakashev, D., Batstone, D.J., Trably, E., Angelidaki, I., 2006. Acetate oxidation is the dominant methanogenic pathway from acetate in the absence of *Methanosaetaceae*. Appl. Environ. Microbiol. 72 (7), 5138–5141.

Keiluweit, M., Nico, P.S., Johnson, M.G., Kleber, M., 2010. Dynamic molecular structure of plant biomass-derived black carbon (biochar). Environ. Sci. Technol. 44 (4), 1247–1253.

Klüpfel, L., Keiluweit, M., Kleber, M., Sander, M., 2014a. Redox properties of plant biomass-derived black carbon (biochar). Environ. Sci. Technol. 48 (10), 5601–5611.

Klüpfel, L., Piepenbrock, A., Kappler, A., Sander, M., 2014b. Humic substances as fully regenerable electron acceptors in recurrently anoxic environments. Nat. Geosci. 7 (3), 195–200.

Lee, J.W., Kidder, M., Evans, B.R., Paik, S., Buchanan III, A.C., Garten, C.T., Brown, R.C., 2010. Characterization of biochars produced from cornstovers for soil amendment. Environ. Sci. Technol. 44 (20), 7970–7974.

Li, J., Hao, X., van Loosdrecht, M.C.M., Luo, Y., Cao, D., 2019. Effect of humic acids on batch anaerobic digestion of excess sludge. Water Res. 155, 431–443.

Lohner, S.T., Deutzmann, J.S., Logan, B.E., Leigh, J., Spormann, A.M., 2014. Hydrogenase-independent uptake and metabolism of electrons by the archaeon *Methanococcus maripaludis*. ISME J. 8 (8), 1673–1681.

Lovley, D.R., 2017. Syntrophy goes electric: direct interspecies electron transfer. Annu. Rev. Microbiol. 71, 643–664.

Lü, F., Luo, C., Shao, L., He, P., 2016. Biochar alleviates combined stress of ammonium and acids by firstly enriching *Methanosaeta* and then *Methanosarcina*. Water Res. 90, 34–43.

Luo, C., Lü, F., Shao, L., He, P., 2015. Application of eco-compatible biochar in anaerobic digestion to relieve acid stress and promote the selective colonization of functional microbes. Water Res. 68, 710–718.

Oh, S.-E., Van Ginkel, S., Logan, B.E., 2003. The relative effectiveness of pH control and heat treatment for enhancing biohydrogen gas production. Environ. Sci. Technol. 37 (22), 5186–5190.

Rotaru, A.-E., Shrestha, P.M., Liu, F., Shrestha, M., Shrestha, D., Embree, M.,

Zengler, K., Wardman, C., Nevin, K.P., Lovley, D.R., 2014a. A new model for electron flow during anaerobic digestion: direct interspecies electron transfer to *Methanosaeta* for the reduction of carbon dioxide to methane. Energy Environ. Sci. 7 (1), 408–415.

Rotaru, A.E., Shrestha, P.M., Liu, F., Markovaite, B., Chen, S., Nevin, K.P., Lovley, D.R., 2014b. Direct interspecies electron transfer between *Geobacter metallireducens* and *Methanosarcina barkeri*. Appl. Environ. Microbiol. 80 (15), 4599–4605.

Shen, Y., Linville, J., Urgun Demirtas, M., Mintz, M., Snyder, S., 2015a. An overview of biogas production and utilization at full-scale wastewater treatment plants (WWTPs) in the United States: challengesand opportunities towards energy-neutral WWTPs. Renew. Sustain. Energy Rev. 50, 346–362.

Shen, Y., Linville, J.L., Urgun-Demirtas, M., Schoene, R.P., Snyder, S.W., 2015b. Producing pipeline-quality biomethane via anaerobic digestion of sludge amended with corn stover biochar with *in-situ* CO_2 removal. Appl. Energy 158, 300–309.

Sieber, J.R., McInerney, M.J., Gunsalus, R.P., 2012. Genomic insights into syntrophy: the paradigm for anaerobic metabolic cooperation. Annu. Rev. Microbiol. 66, 429–452.

Stams, A.J., Plugge, C.M., 2009. Electron transfer in syntrophic communities of anaerobic bacteria and archaea. Nat. Rev. Microbiol. 7 (8), 568–577.

Storck, T., Virdis, B., Batstone, D.J., 2016. Modelling extracellular limitations for mediated versus direct interspecies electron transfer. ISME J. 10 (3), 621–631.

Sun, T., Levin, B.D., Guzman, J.J., Enders, A., Muller, D.A., Angenent, L.T., Lehmann, J., 2017. Rapid electron transfer by the carbon matrix in natural pyrogenic carbon. Nat. Commun. 8, 14873.

Sun, T., Levin, B.D.A., Schmidt, M.P., Guzman, J.J.L., Enders, A., Martinez, C.E., Muller, D.A., Angenent, L.T., Lehmann, J., 2018. Simultaneous quantification of electron transfer by carbon matrices and functional groups in pyrogenic carbon. Environ. Sci. Technol. 52 (15), 8538–8547.

Wang, T., Zhang, D., Dai, L., Dong, B., Dai, X., 2018. Magnetite triggering enhanced direct interspecies electron transfer: a scavenger for the blockage of electron transfer in anaerobic digestion of high-solids sewage sludge. Environ. Sci. Technol. 52 (12), 7160–7169.

Xu, S., Adhikari, D., Huang, R., Zhang, H., Tang, Y., Roden, E., Yang, Y., 2016. Biochar-facilitated microbial reduction of hematite. Environ. Sci. Technol. 50 (5), 2389–2395.

Xu, W., Pignatello, J.J., Mitch, W.A., 2013. Role of black carbon electrical conductivity in mediating hexahydro-1,3,5-trinitro-1,3,5-triazine (RDX) transformation on carbon surfaces by sulfides. Environ. Sci. Technol. 47 (13), 7129–7136.

Xu, Y., Lu, Y., Dai, X., Dong, B., 2017. The influence of organic-binding metals on the biogas conversion of sewage sludge. Water Res. 126, 329–341.

Yuan, H.Y., Ding, L.J., Zama, E.F., Liu, P.P., Hozzein, W.N., Zhu, Y.G., 2018. Biochar modulates methanogenesis through electron syntrophy of microorganisms with ethanol as a substrate. Environ. Sci. Technol. 52 (21), 12198–12207.

Zhao, Y., Chen, Y., Zhang, D., Zhu, X., 2010. Waste activated sludge fermentation for hydrogen production enhanced by anaerobic process improvement and acetobacteria inhibition: the role of fermentation pH. Environ. Sci. Technol. 44 (9), 3317–3323.

Zhao, Z., Li, Y., Quan, X., Zhang, Y., 2017a. Towards engineering application: potential mechanism for enhancing anaerobic digestion of complex organic waste with different types of conductive materials. Water Res. 115, 266–277.

Zhao, Z., Zhang, Y., Holmes, D.E., Dang, Y., Woodard, T.L., Nevin, K.P., Lovley, D.R., 2016a. Potential enhancement of direct interspecies electron transfer for syntrophic metabolism of propionate and butyrate with biochar in up-flow anaerobic sludge blanket reactors. Bioresour. Technol. 209, 148–156.

Zhao, Z., Zhang, Y., Li, Y., Dang, Y., Zhu, T., Quan, X., 2017b. Potentially shifting from interspecies hydrogen transfer to direct interspecies electron transfer for syntrophic metabolism to resist acidic impact with conductive carbon cloth. Chem. Eng. J. 313, 10–18.

Zhao, Z., Zhang, Y., Yu, Q., Dang, Y., Li, Y., Quan, X., 2016b. Communities stimulated with ethanol to perform direct interspecies electron transfer for syntrophic metabolism of propionate and butyrate. Water Res. 102, 475–484.

Zhou, G.W., Yang, X.R., Li, H., Marshall, C.W., Zheng, B.X., Yan, Y., Su, J.Q., Zhu, Y.G., 2016. Electron shuttles enhance anaerobic ammonium oxidation coupled to iron(III) reduction. Environ. Sci. Technol. 50 (17), 9298–9307.